Proceedings of the 6th European VLBI Network Symposium
Ros, E., Porcas, R.W., Lobanov, A.P., & Zensus, J.A. (eds.)
June 25th-28th 2002, Bonn, Germany

Simultaneous 3mm and 7mm Observations of SiO Masers around R Cassiopeiae: The Maser Line Ratios

R. B. Phillips[1], A. H. Straughn[2⋆], C.J. Lonsdale[1], and S. S. Doeleman[1]

[1] MIT Haystack Observatory, Westford, MA 01886, USA
[2] University of Arkansas, Fayetteville, AR 72701 , USA

Abstract. We present dual-transition ($J = 1 \rightarrow 0$ and $J = 2 \rightarrow 1$) images for R Cassiopeiae. Line ratios and limits for the $J = 1 \rightarrow 0$ and $J = 2 \rightarrow 1$ emission vary from roughly unity to several hundred to one. Local velocity trends can be seen in the VLBI images. These new, specific comparisons of rotational transitions show promise for testing emission models, and should be used to incisively probe the physical processes at the base of AGB star mass-loss envelopes.

1. Introduction

SiO maser rings around cool giant and supergiant stars have been described by Diamond et al.(1994), Greenhill et al.(1995), Kemball & Diamond(1997), Boboltz et al.(1997), Desmurs et al.(2000), Hollis et al.(2000), Yi et al. (2000), Hollis et al.(2001) for the $J = 1 \rightarrow 0$ masers near 43 GHz, and by Doeleman et al.(1998) and Phillips et al.(2001) for the $J = 2 \rightarrow 1$ masers near 86 GHz. These studies employed either the Very Long Baseline Array (VLBA)[1] for the $J = 1 \rightarrow 0$ SiO masers near 43 GHz, or the Coordinated mm-VLBI Array (CMVA)[2] for the $J = 2 \rightarrow 1$ masers near 86 GHz. Simultaneous observing at 43 and 86 GHz was not done in any of the VLBI studies. Before 2001, there was no practical way to observe these two families of bright SiO masers simultaneously with VLBI.

The literature leaves a fragmented record of maser envelope morphology, variability, and velocity structure. Except for the "movie" project of Diamond & Kemball (1999), SiO maser images were made across an arbitrary selection of stars and stellar pulsation phases. Previous VLBI work on R Cassiopeiae (R Cas), a normal red giant at a distance ∼160 AU, established that both its 86 and 43 GHz SiO masers arise in a spotty ring and vary greatly from year to year (Yi et al. (2000), Phillips et al.(2001)). Diamond & Kemball (1999) made VLBA images of the $J = 1 \rightarrow 0$ masers around TX Camelopardalis (TX Cam) with monthly or better time coverage. Their maser movies vividly show apparent proper motions, including both outflow- and infall-like motions. In parallel, Gray & Humphreys(2000) and Humphreys et al.(2002) developed models that qualitatively reproduced the $J = 1 \rightarrow 0$ maser ring of TX Cam, but also predicted the appearance of the poorly documented $J = 2 \rightarrow 1$ masers.

In the spring 2001 observing season, operational 86 GHz capability became available on the VLBA. This upgrade to the VLBA provided the critically important option to observe both $J = 1 \rightarrow 0$ and $J = 2 \rightarrow 1$ masers by switching between 43 and 86 GHz. We present our first results from this mode, register the two lower rotational transitions, and discuss implications for evaluating emission models.

2. Observations

We observed R Cas on 2001 April 27 as part of the VLBA's inaugural season of 86 GHz programs. Our goal was to explore the VLBA capability for simultaneous 43/86 GHz maser imagery, and only one twelve-hour track was scheduled. R Cas was at stellar photometric phase 0.54 relative to measured maximum.

The VLBA was outfitted with 86 GHz receivers only on the inner half of the array. As a result, u, v coverage at 43 and 86 GHz was nearly identical in extent, yielding scaled-array observations for the two SiO transitions (Figure 1). The data were correlated in Socorro, New Mexico at the VLBA correlator to yield a spectral resolution of 0.44 km s^{-1} at 43 GHz and 0.22 km s^{-1} at 86 GHz. Standard sequential approaches to calibrate fringe delay, receiver bandpasses, and amplitudes were employed before fringe-fitting to suitable reference features. Total power spectra from the VLBI autocorrelations for the $J = 1 \rightarrow 0$ and $J = 2 \rightarrow 1$ transitions are shown in Figure 2. The total power spectra were translated to flux density using logged receiver and antenna performance for an optimal elevation scan at the Kitt Peak VLBA telescope. Amplitude calibration was then transferred to the remainder of the observations by registering all antenna auto-spectra to this template scan every two minutes. The

⋆ MIT Haystack Observatory Research Experience for Undergraduates Program

[1] The National Radio Astronomy Observatory is a facility of the National Science Foundation, operated under a cooperative agreement by Associated Universities, Inc.

[2] The CMVA is operated through Haystack Observatory under support from the NSF.

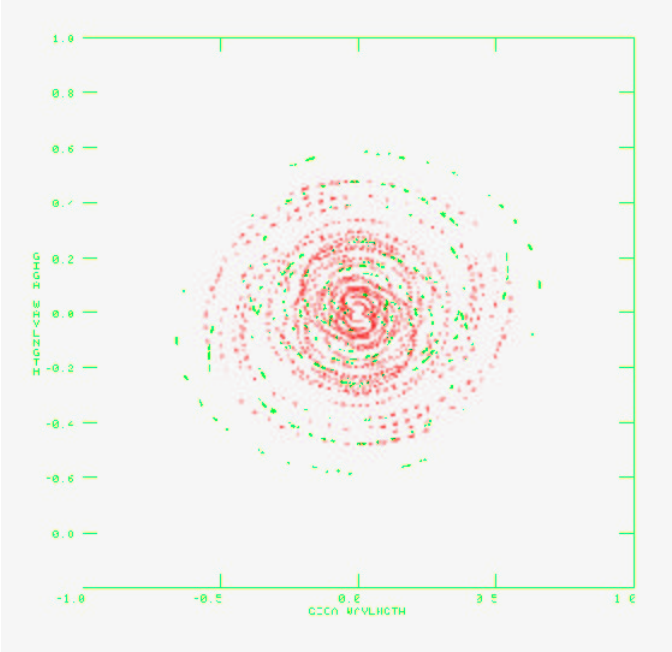

Fig. 1. u,v coverage of 43 GHz $J = 1 \rightarrow 0$ data (grey) and 86 GHz $J = 2 \rightarrow 1$ data (black).

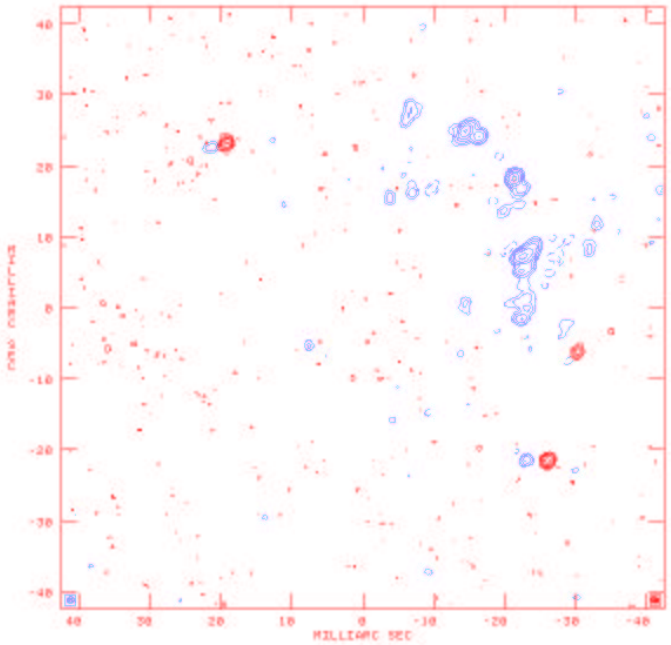

Fig. 2. Maps of $J = 1 \rightarrow 0$ (grey) and $J = 2 \rightarrow 1$ (black), integrated across all velocity channels observed; $J = 2 \rightarrow 1$ offset 3 beam FWHM to west.

template method corrects for atmospheric attenuation and telescope pointing, critical to achieving proper amplitude calibration at 86 GHz.

Image cubes were made for the 43 and 86 GHz lines over a common Doppler velocity range. Both sky images, integrated or "squashed" over all spectral channels, are shown in Figure 2. The two transitions are shown with $J = 2 \rightarrow 1$ offset to the west from $J = 1 \rightarrow 0$ by three beam FWHM to visually separate the contours.

The 86 GHz masers were anomalously faint for a stellar phase of 0.54, which should correspond to an SiO emission phase of 0.24 to 0.34 (Martínez et al.(1998)). While the 43 GHz emission showed a peak of 1800 Jy (spectral resolution of 0.44 km s^{-1}), the 86 GHz masers showed a multi-lined spectrum whose two strongest features were 60 Jy (0.22 km s^{-1} resolution). We expected the weakness of the 86 GHz masers to compromise imaging, but the compactness of SiO masers permitted us to detect and model a reference feature (the solitary maser clump near position angle $-135°$), and to image the three bright spots seen in Figure 3. In the channel containing the peak of this bright 86 GHz maser, self-calibration approaches yielded a best map whose dynamic range, limited by close-in side-lobe artifacts, is 10:1. Map noise well away from the reference maser gives a more favorable but unrealistic value of 90:1. Nearly identical dynamic ranges result for the channels containing the other bright features, so the dynamic range of 10:1 can be adopted for all of the 86 GHz image.

For the more maser-rich 43 GHz emission, SNR much superior to that at 86 GHz resulted in the dynamic range limit being roughly a tie between off-source RMS noise and beam-like artifacts. A few bright channels of the complex maser arc in p.a. $-45°$ to $-90°$ have dynamic ranges of 15 to 20:1, but a more typical value for channels with significant emission is 30:1.

3. Line ratios

These two bright rotational transitions can be trivially registered via two "anchor points": the bright maser clumps that occur near p.a $45°$ and $-135°$ occupy the same velocities in both transitions. In the 43 GHz and 86 GHz images, the masers at p.a $45°$ had fitted velocities of 25.5 km s^{-1} The 43 GHz maser spot at p.a.$-135°$ was visible in two channels, spanning 24.3 to 24.7 km s^{-1}, while the 86 GHz image had corresponding emission only in its 24.5 km s^{-1} channel. We adopted a sky centroid interpolated between these two 43 GHz channels, then registered the 86 and 43 GHz maser images.

Line ratios between $J = 1 \rightarrow 0$ and $J = 2 \rightarrow 1$ can be derived for coincident emission, and lower limits estimated where one or the other transition is absent from the image. A composite of line ratios and limits is shown in Figure 3. The results have been convolved to twice the beam size to suppress edge effects around components. Values range from roughly 0.7:1 (two regions used in registration) to lower limits of 300:1 (maser arc to the northwest).

This epoch is probably a poor example to begin with if extensive comparisons of line ratios with models are to be attempted, since the $J = 2 \rightarrow 1$ masers were anomalously weak. However, our line ratios and limits are a demonstration of current VLBI capabilities meant to exhort investigators to exploit such SiO measurements aggressively.

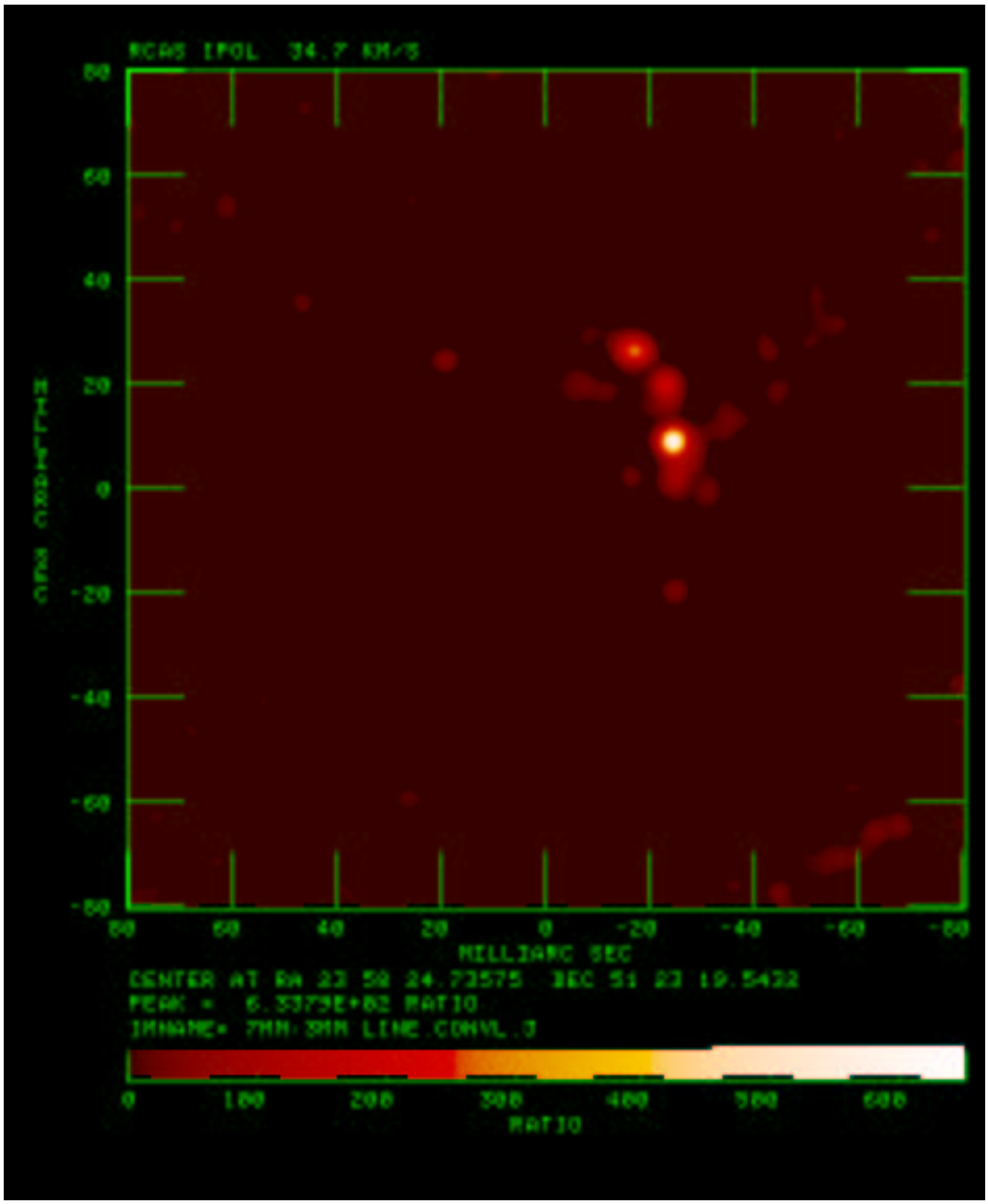

Fig. 3. Line ratios and limits on ratios, $J = 1 \rightarrow 0$ to $J = 2 \rightarrow 1$. Results convolved to two beam widths to suppress edge effects.

4. Possible Rotation?

In recent literature (Boboltz et al.(2000), Hollis et al.(2000), Hollis et al.(2001)) examples of apparent shell rotation have been reported for the stars NML Cygni and R Aquarii. In the $\sim 45°$ arc of bright masers to the northwest of R Cas in $J = 1 \rightarrow 0$ ring, there is a monotonic gradient in Doppler velocity of 0.5 km s^1 AU^{-1} over about 5 AU. Although this arc might be construed as a section of a rotating envelope, regional velocity ordering has been seen in the masers of R Cas before (Phillips et al.(2001)). This grouping of 43 GHz masers may reflect merely another such regional velocity grouping aligned along the shell, rather than shell rotation. Other epochs of R Cas observed to date have not shown any visible evidence for shell rotation (Yi et al. (2000), Phillips et al.(2001)).

5. Comparison of Maser Transitions and Model Predictions

Humphreys et al.(2002)
have developed a model in which pulsation-driven shocks trigger local clumping and velocity conditions favorable or not for masing. The model predicts the general character

of the $J = 1 \rightarrow 0$ rings at 43 GHz through a pulsation cycle, and also the relative location and strength of the $J = 2 \rightarrow 1$, $v = 1$ masers at 86 GHz. Our new single-epoch results, which ought to correspond to their model (not stellar) phase 0.30 to 0.35[3], can be compared to predictions.

• R Cas appears to show a 86 GHz ring that is (1) weaker than 43 GHz overall, and (2) had faded nearly to invisibility. Humphreys et al.(2002) predict (2), but the opposite of (1). The model 86 GHz masers are brighter at most phases except for 86 GHz minimum, which these observations may have observed if it arrived earlier than normal in this cycle.

• A few bright maser features at 86 GHz compose the total $v = 1$, $J = 2 \rightarrow 1$ spectrum, and two of these are brighter than the corresponding 43 GHz $v = 1$, $J = 1 \rightarrow 0$ masers. Two maser components appear in both transitions, but a much larger fraction do not. However, this result suggests that bright 86 GHz $v = 1$ masers form under the same conditions as the 43 GHz $v = 1$ masers. Humphreys et al.(2002) model results predict that the 86 GHz masers will generally be a subfamily of those at 43 GHz.

• The very spartan $v = 1$ 86 GHz ring appears to register with the $v = 1$ 43 GHz ring. If the location of the two maser features in common between 86 GHz and 43 GHz reflect ring size, the two $v = 1$ rings have comparable radii. Nearly equal $v = 1$ ring radii are predicted by Humphreys et al.(2002).

• An anomalous red 43 GHz maser appears over the likely location of the stellar disk. Masing locations other than the canonical tangential gain paths around the circumference of the star probably mark local density enhancements with tight velocity ordering. Occasional disk masers also emerged from the model of Humphreys et al.(2002), where pulsation-driven shocks create clumping in the model envelope.

Our single-epoch comparison of transitions is thus more often consistent with the predictions of Humphreys et al.(2002) than not. Since Humphreys et al.(2002) developed their model in the absence of inputs from 86 GHz maser VLBI, the favorable match may reflect the soundness of their physical assumptions. Humphreys et al.(2002) currently hold the radiative part of their pump constant, and a more realistic underlying star may shift maser variations in the cycle. The aspects where differences between our images and Humphreys et al.(2002) are sharpest, such as the amplitude and detailed timing of maser variations, might also be expected to vary substantially from one AGB star to another. The SiO masers of R Cas appeared more like model frame 9 or 10 of Humphreys et al.(2002), with 86 GHz much weaker than 43 GHz. Thus, R Cas may fit well in the Humphreys et al.(2002) model, but pulsation-driven shocks may have arrived 0.1 to 0.2 periods early at the masing region compared to their model.

[3] The model of Humphreys et al.(2002) was computed at 20 epochs or frames spanning a stellar pulsation cycle; these VLBI observations translate to their frame 6 or 7.

6. Conclusions

Our SiO VLBI observations have registered the $J = 1 \rightarrow 0$ and $J = 2 \rightarrow 1$ masers of the $v = 1$ state. Rotational states in the same vibrational rung appears to be at least as diverse as vibrational states within a given J number rotational state, as a comparison with Desmurs et al.(2000) and Yi et al. (2000) will demonstrate. Results for the first two bright rotational transitions thus far support the stellar SiO maser model of Humphreys et al.(2002). These new VLBI images do not select a preferred mode (radiative over collisional) for maser pumping.

The VLBA is a viable instrument for observing bright SiO masers near 86 GHz, and spatial registration of the different ro-vibrational SiO masers of AGB stars should soon become commonplace. This limited demonstration of dual-SiO-line VLBI has shown that simultaneous VLBA observing at 43 and 86 GHz can be an effective input to SiO maser emission modeling. Future VLBI studies of SiO masers near AGB stars should be scheduled so that both $J = 1 \rightarrow 0$ and $J = 2 \rightarrow 1$ lines are imaged.

References

Boboltz, D. A., Diamond, P. J., and Kemball, A. J. 1997, ApJ, 487, L147
Boboltz, D. A., & Marvel, K. B. 2000, ApJ, 545, L149
Desmurs, J. F., Bujarrabal, V., Colomer, F., & Alcolea, J. 2000, A&A, 360, 189
Diamond, P. J., Kemball, A. J., Junor, W., et al. 1994, ApJ, 430, L61
Diamond, P. J., & Kemball, A. J. 1999, in Asymptotic Giant Branch Stars, ed. T. Le Bertre, A. Lebre, & C. Waelkens IAUS, 191, 195
Doeleman, S.S., Lonsdale, C.J., & Greenhill, Lincoln J., 1998, ApJ, 494, 400
Gray, M. D., & Humphreys, E. M. L. 2000, New Astronomy Reviews, 5, 155
Greenhill, L. J., Colomer, F., Moran, J. M., et al. 1995, ApJ, 449, 365
Hollis, J. M., Pedelty, J. A., Forster, J. R., et al. 2000, ApJ, 543, L81
Hollis, J. M., Boboltz, D. A., Pedelty, J. A., White, S. M., & Forster, J. R. 2001, ApJ, 559, L37
Humphreys, E. M. L., Gray, M. D., Yates, J. A., et al. 2002, To appear in A&A
Kemball, A. J., & Diamond, P. J. 1997, ApJ, 481, L111
Martínez, A., Bujarrabal, V., & Alcolea, J. 1988, A&AS, 74, 273
Phillips, R. B., Sivakoff, G. R., Lonsdale, C. J., & Doeleman, S. S. 2001, AJ, 122, 2679
Yi, J., Booth, R. S., Conway, J. E., Diamond, P., & Winnberg, A. 2000, in Proceedings of the 5th European VLBI Network Symposium, ed. J.E. Conway, A.G. Polatidis, R.S. Booth & Y.M. Pihlstrom, published Onsala Space Observatory